Solar Phys (2008) 247: 203–216
DOI 10.1007/s11207-007-9070-y

Total Solar Irradiance Measurement and Modelling during Cycle 23

S. Mekaoui · S. Dewitte

Received: 7 December 2006 / Accepted: 5 October 2007 / Published online: 6 December 2007

Abstract During solar cycle 23, which is now close to its end, variations of the total solar irradiance were measured by six different instruments, providing four independent time series of the irradiance variation over the complete solar cycle. A new composite time series constructed using five of these six instruments provides unprecedented instrument stability for the study of the open question of solar irradiance variations between minima. An independent analysis of the different composite time series is performed through an empirical proxy model fit. The new composite is fitted with 0.96 correlation ($R^2 = 93\%$) and RMS error of 0.15 W m^{-2}, thus reaching the limit of the individual instrument stabilities. Both the measurements and the model indicate that for the current cycle the minimum irradiance level has not yet been reached. Therefore we use the model to extrapolate measurements up to 2008 when the minimum irradiance level is expected. If we assume that there will be no changes in the solar irradiance from 2006 to 2008 that are not captured by the regression model, it can be predicted that there will be no variation of the solar minimum irradiance level during cycle 23 with an uncertainty of ± 0.14 W m^{-2}.

Keywords TSI variability · TSI composites · Magnetic indices

1. Introduction

Total solar irradiance (TSI) has been monitored from space for more than 25 years with different radiometers. In time, the number and quality of the radiometers have increased, allowing improvement of the long-term stability of the measurements. A critical question

S. Mekaoui (✉) · S. Dewitte
Royal Meteorological Institute of Belgium, Ringlaan 3, 1180 Brussel, Belgium
e-mail: sabri.mekaoui@oma.be

S. Dewitte
e-mail: steven.dewitte@oma.be

S. Mekaoui
Vrije Universiteit Brussel, Pleinlaan 2, 1050 Brussel, Belgium

is whether TSI variations on time scales longer than 11 years – which would be the most relevant for climate changes on Earth – exist. Such changes would be visible as changes of the TSI level between solar minima.

Spanning the previous solar cycle 22, three composite time series are available. They exhibit different behaviour, mainly between the last two solar minima (Fröhlich and Lean, 1998; Willson and Mordvinov, 2003; Dewitte *et al.*, 2005). The differences in solar minima variations among the three composites can be attributed to the different interpretation of the available instruments' data during the so-called ACRIM gap period when only two instruments without degradation monitoring channels were available, resulting in an uncertainty of ± 0.35 W m^{-2} of the minimum TSI variation.

For the current solar cycle 23, which is coming close to its end, the situation is much better, with a TSI measurement by six independent instruments, of which five have ageing monitoring channels, providing four independent measurement series over the complete solar cycle. We will exploit this opportunity by constructing a new space absolute radiometric reference (SARR) composite time series, as an update of the one from Dewitte *et al.* (2005), with the aim of representing the TSI variation during cycle 23 as accurate as possible.

On time scales from days to the 11-year solar activity period, it is known that the major contributions to the irradiance variations come from dark sunspots and bright features on the solar disc. Both are characterized by an increased magnetic-field strength compared to the solar disc background; hence they can be called magnetic features. The current TSI proxy models use these features as the two "magnetic" ingredients to reconstruct the measured TSI variation from 1978 to 2006. De Toma *et al.* (2004) particularly use the Mg II index from Viereck *et al.* (2001) as a bright-feature index and the Σ_{red} index from the San Fernando Observatory as a dark-sunspot index (Preminger, Walton, and Chapman, 2002; Walton *et al.*, 2004). Here we extend the applied method to the ACRIM, PMOD, and the new Royal Meteorological Institute of Belgium (RMIB) SARR composite by adding a third proxy component to the model: the magnetic-plage strength-index (MPSI) from the Mount Wilson Observatory. We first introduce the different composite TSI time series and we derive a new RMIB time series in Section 2. We then describe the different proxy indices in Section 3 and introduce the model equation in Section 4. In Section 5 we determine an empirical model fit over solar cycle 23 for each of the composites and calculate the associated residual errors. We then select the best model fit based on the minimal RMS error between the measurements and the model as well as the maximal coefficient of determination. Finally, we compute the estimated total solar irradiance for solar cycle 22 and compare it with the measurements in Section 6. We end with conclusions.

2. TSI Composite Time Series

Different total solar irradiance composite time series have been proposed and show some substantial differences. Here we use the daily averaged TSI values of each composite and focus on their respective behaviour between the last two solar minima (see Figure 1 and references hereafter for more details).

- *The Active Cavity Radiometer Irradiance Monitor (ACRIM) composite version 11/06* (Willson and Mordvinov, 2003): The composite has been updated. It is characterized by an increase of the Quiet-Sun irradiance level of 0.037% per decade (*i.e.*, about 0.5 W m^{-2} between the last two minima (21 and 22)) and a decrease of 0.025% per decade between solar cycle 22 and 23 minima.

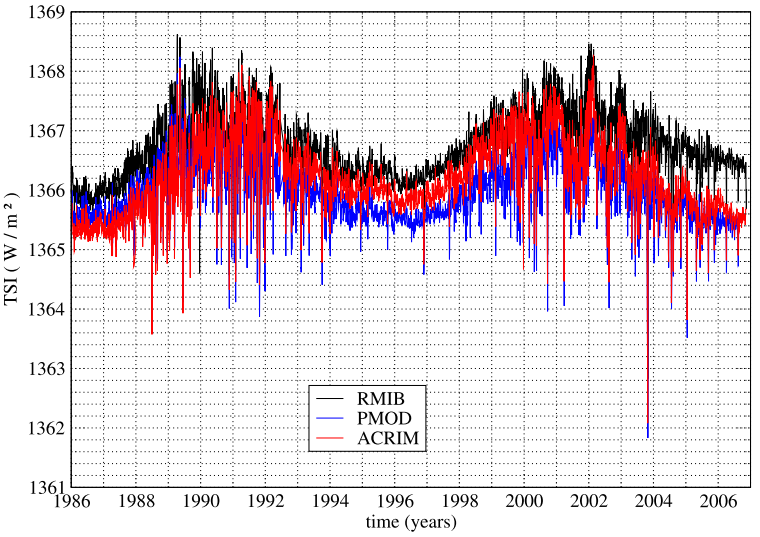

Figure 1 The three different TSI composite time series as a function of time as compiled by their respective authors.

- *The Physikalisch-Meteorologisches Observatorium Davos (PMOD) composite version d41610608* (Fröhlich and Lean, 1998): Besides the correction for exposure-dependent ageing, this composite accounts for other instrument's degradations and the influence of operational interruptions (Fröhlich, 2004). The compiled composite has no minimum-to-minimum trend. The composite has been updated (Foukal *et al.*, 2006).
- *The RMIB or SARR composite*: This composite is an update from the one compiled in Dewitte *et al.* (2005). We use the daily averaged TSI data from the following instruments:
  - *Differential Absolute Radiometer (DIARAD) data* (Crommelynck, 1982; Crommelynck and Domingo, 1984): The DIARAD radiometer developed at the Royal Meteorological Institute of Belgium operates on SOHO as part of the VIRGO experiment. The on-orbit ageing correction of DIARAD is obtained only from the comparison of its own two channels. Compared to the version of Dewitte, Crommelynck, and Joukoff (2004) we have improved the determination of the reference-cavity shutter temperature. This modification will be documented in a separate paper.
  - *PMOV06 data*: PMOV06 is composed of two radiometers: PMOV06-A and PMOV06-B. PMOV06-A measures the Sun routinely; PMOV06-B is used from time to time to verify the ageing of PMOV06-A. Here we want to use PMOV06 as an independent data set. We therefore correct PMOV06-A for its ageing by comparison with PMO06-B in a similar way as we have corrected DIARAD left for ageing with DIARAD right.

    Alternative PMOV06 and DIARAD TSI time series are available from Fröhlich (2003). In this paper, the so-called level 1.8 is comparable to our ageing-corrected TSI time series. The so-called level 2 considers additional "exposure-independent" corrections.
  - *ACRIM 2 and ACRIM 3 data*: We used the data available from www.acrim.com. For ACRIM 2, we use version 3; for ACRIM 3 we use version 11/06.
  - *Earth Radiation Budget Satellite (ERBS) data*: The solar monitor on ERBS is a radiometer with a relatively high noise level, partly because of its sparse sampling, which

Table 1 SARR adjustment coefficients used.

Instrument	SARR adjustment coefficient
DIARAD	1.000295
PMO06	1.000690
ACRIM 2	1.001667
ACRIM 3	1.000294
TIM	1.004195
ERBS	1.000917

allows us to assume a low exposure-dependent ageing, even if there is no ageing monitoring channel to verify this. Despite the noise, which affects the short-term variations measured by ERBS, it provides useful measurements of the long-term variations of the TSI, which are independent of those of the other radiometers.

We define a denoised version of the ERBS irradiance, $S_E(t)$, given by

$$S_E(t) = m_{21}\left[S_{E,0}(t) - S_{\text{comp}}(t)\right] + S_{\text{comp}}(t), \tag{1}$$

where $S_{E,0}(t)$ is the original – noisy – ERBS measurement, $S_{\text{comp}}(t)$ is the composite time series of all radiometers except ERBS, and m_{21} denotes the running mean over 21 ERBS measurements. Equation (1) assures that $S_E(t)$ has the long-term behaviour of ERBS and the short-term – low-noise – behaviour of $S_{\text{comp}}(t)$.

– *Total Irradiance Monitor (TIM) data*: The total irradiance monitor has operated on the *Solar Radiation and Climate Explorer* (SORCE) satellite since early 2003. We used version 7 available from http://lasp.colorado.edu/sorce.

All instruments are brought to the same absolute level by multiplication with an instrument-specific SARR adjustment coefficient, given in Table 1.

Figure 2 shows the 121-day running mean of all SARR-adjusted time series during cycle 23. The level of the irradiance in 2006 (see the blue curve in Figure 3) is 0.3 to 0.4 W m^{-2} higher than the level in 1996. This could suggest that there has been a decadal change between 1996, which corresponds to the end of the previous solar minimum, and 2006, which is close to the new minimum. A comparison with a regression model to be introduced in the next section (see black curve in Figure 2) will indicate that the higher level in 2006 occurs because the minimum irradiance level has not been reached yet, and not because of a decadal minimum level TSI change.

The TSI variations of the different instruments agree well, with the exception of ACRIM3, which descends more rapidly than the other radiometers.

By averaging different instruments, instrumental errors of one single instrument are strongly suppressed. Figure 3 shows the 121-day running mean of the composite time series obtained by averaging, respectively, only the VIRGO radiometers DIARAD and PMOV06, only the ACRIM2, ERBS, and TIM measurements, and finally all of those together.

The VIRGO composite shown here differs from the one of Fröhlich (2003), which corrects for non-exposure-dependent instrument changes. These changes – if they exist – become negligible in the overall composite because of the aforementioned averaging effect.

An upper limit of the "internal error" of the overall composite – indicative of the internal consistency of the individual components that contribute to the composite – can be obtained by taking the difference of the partial VIRGO and ACRIM2-ERBS-TIM composites, shown as the red curve in Figure 4.

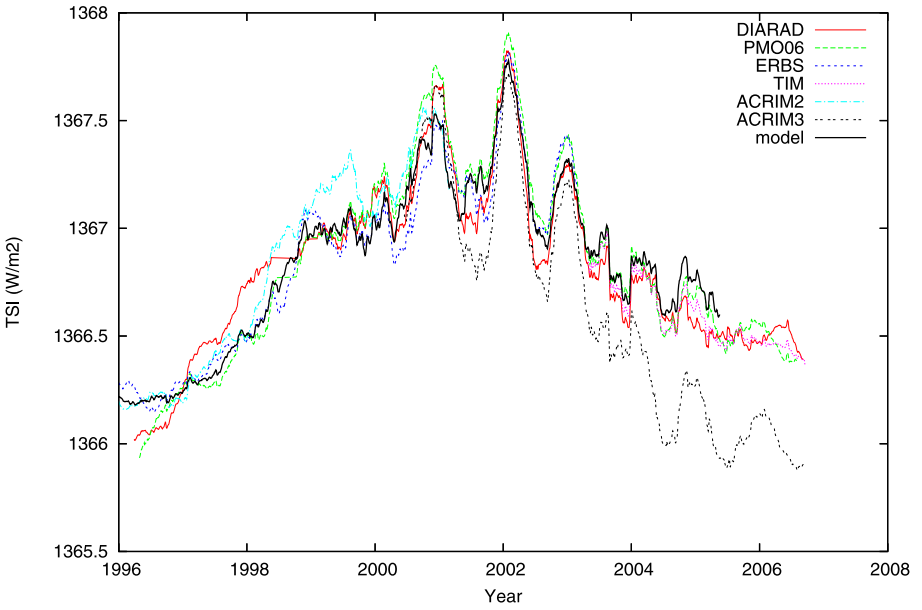

Figure 2 The 121-day running mean of the TSI measurements of individual instruments. Red curve: DIARAD/VIRGO measurements; green curve: PMOV06/VIRGO measurements; dark blue curve: denoised ERBS measurements; purple curve: TIM measurements; light blue curve: ACRIM2 measurements; dashed black curve: ACRIM3 measurements; full black curve: empirical proxy model for RMIB composite.

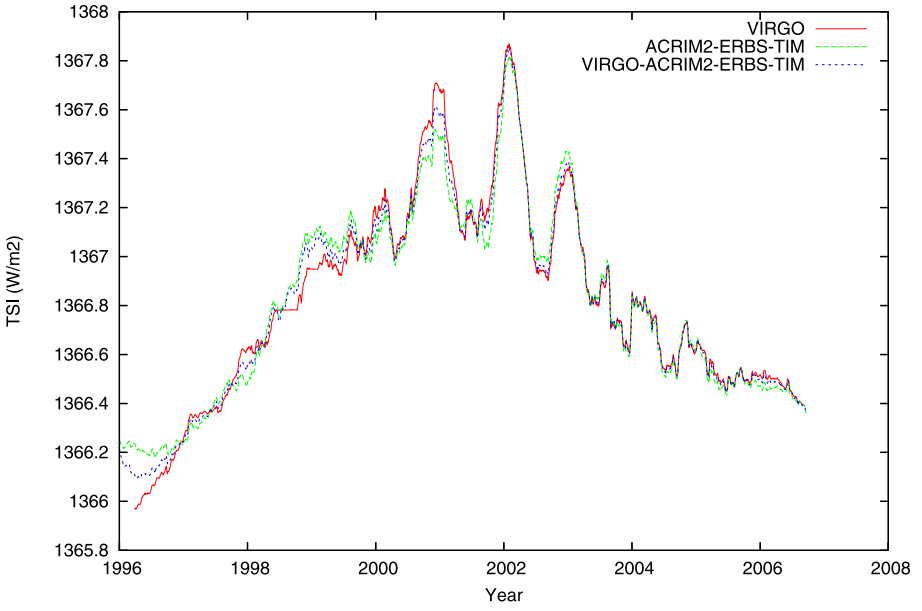

Figure 3 The 121-day running mean of different composites of SARR-adjusted TSI measurements. Red curve: composite of DIARAD/VIRGO and PMOV06/VIRGO measurements; green curve: composite of ACRIM2, denoised ERBS, and TIM measurements; blue curve: composite of DIARAD/VIRGO, PMOV06/VIRGO, ACRIM2, denoised ERBS, and TIM measurements.

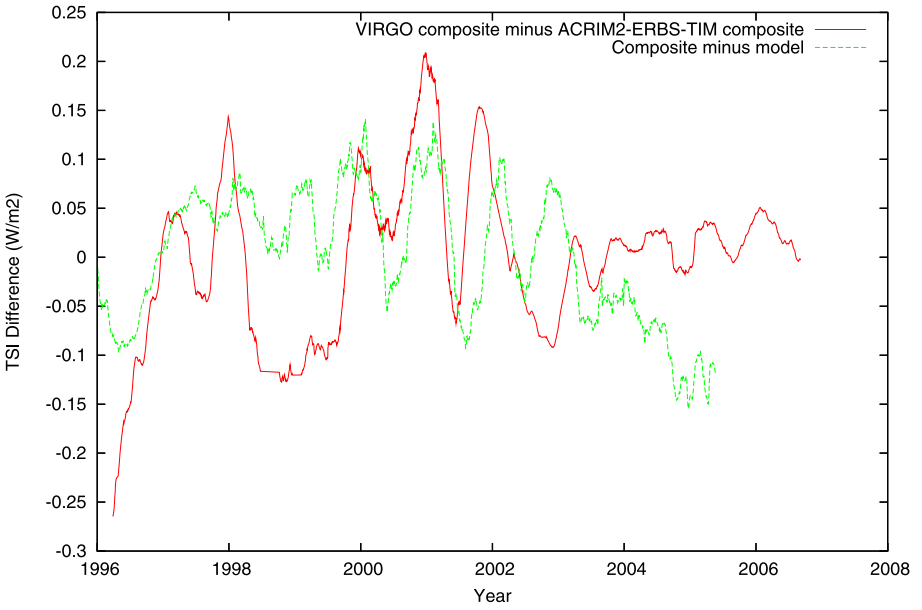

Figure 4 The 121-day running mean of TSI differences. Red curve: VIRGO composite minus ACRIM2-ERBS-TIM composite; green curve: overall RMIB composite minus RMIB regression model.

The difference is mostly within ± 0.2 W m^{-2} during the first part of the solar cycle and is within ± 0.05 W m^{-2} from 2003 onwards. The year 2003 corresponds both to the start of the TIM measurements and to the start of the final declining phase of the TSI after the three big maxima of cycle 23 (see Figure 3).

3. Proxy Indices

Different indices for modeling the TSI long-term variability have been proposed (De Toma *et al.*, 2004). They exist for different periods of time, therefore limiting their use for empirical TSI reconstruction to the period of their availability. These indices take into account the Sun's variability in different wavelengths. For the current study we have used the following:

- *The* Σ_{red} *index*: This index is a sum over all image pixels from the Cartesian full-disc telescope at San Fernando Observatory (Figure 5). This index is derived from radiation formed in the photosphere. It is obtained using red filtergrams at 672.3 nm and 10 nm bandpass. It is representative of the short-term darkening effect of sunspots on the solar irradiance (Preminger, Walton, and Chapman, 2002; Walton *et al.*, 2004; Walton, 2005, private communications).
- *The Mg* II *index*: The Mg II core-to-wing ratio index (Figure 6) is derived from spectroscopic UV irradiance measurements around 280 nm (Viereck, Puga, and Lawrence, 1999; Viereck *et al.*, 2001). This index is sensitive to solar bright regions. From Figure 6 we can assume the Mg II index will reach the same level as during the previous solar irradiance minimum.
- *The MPSI index*: The MPSI index is derived from ground-based magnetograms using the Mount Wilson solar tower telescope (Figure 7). This index is computed by summing the

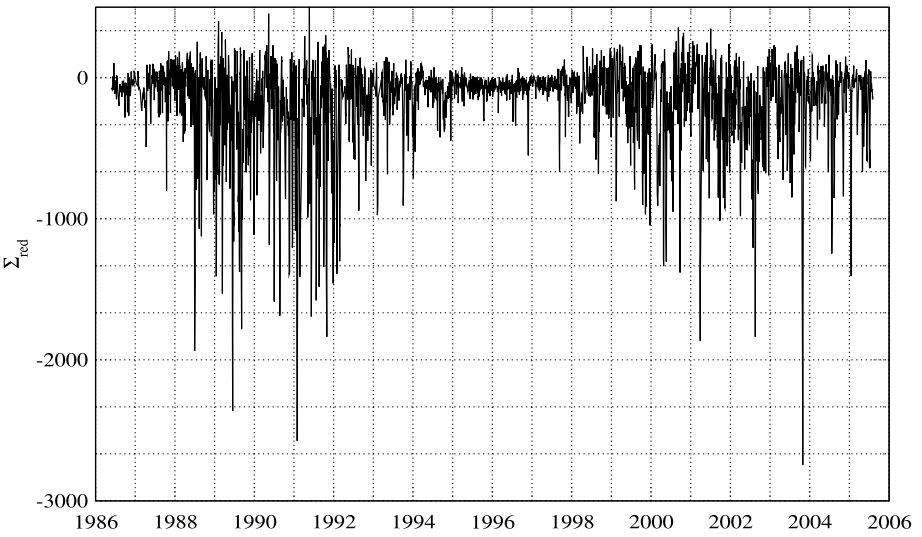

Figure 5 The Σ_{red} index as a function of time from Walton (2005, private communications).

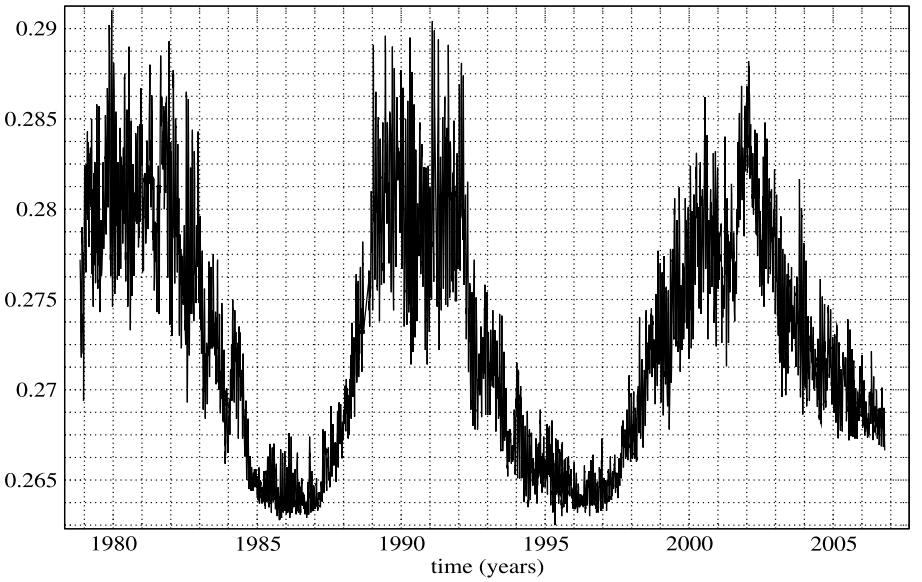

Figure 6 The Mg II core-to-wing ratio as a function of time.

values of the magnetic field strength for all of the pixels where the absolute value lies between 10 and 100 gauss. This summation is then divided by the total number of pixels regardless of the pixel's value.

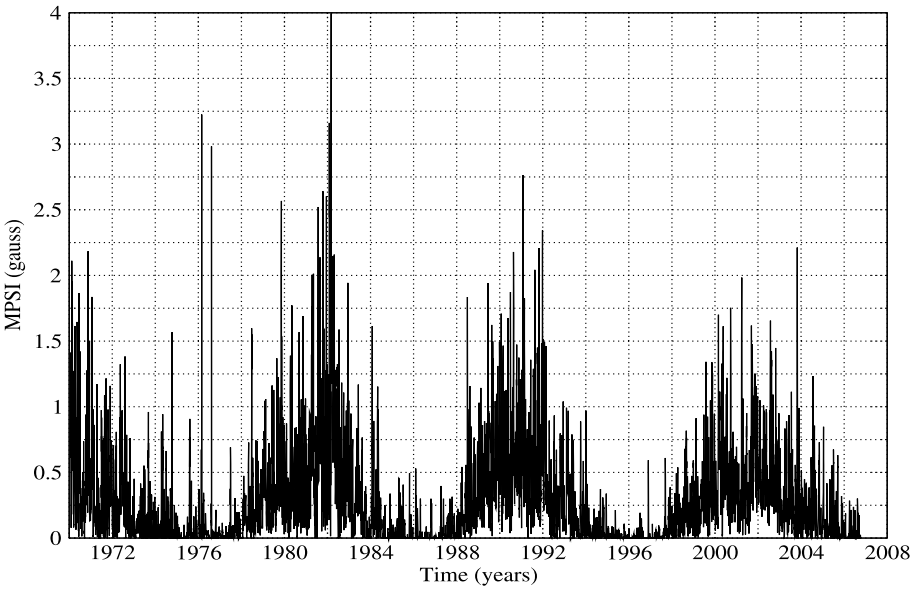

Figure 7 The magnetic plage strength index.

4. Magnetic Model Determinations for Solar Cycle 23

Using the Mg II, $\Sigma_{\rm red}$, and MPSI indices covering solar cycle 23, we determine for each of the TSI composite time series a least-square-fit model. This model is introduced to check whether this irradiance level difference (Figure 2) is due to long-term minima changes or to the fact that the current minimum has not been reached yet. This empirical model should reproduce the TSI variation with fidelity. We have therefore selected a model of the form

$$\mathrm{TSI}_i(t) = a + b\Sigma_{\rm red}(t) + c\mathrm{Mg\,II}(t) + d\mathrm{MPSI}(t), \tag{2}$$

where i means, consecutively, the RMIB, ACRIM, and PMOD composites time series, t is the time in days, and a, b, c, and d are the coefficients to be determined. Note that we correct all indices by their respective mean value for the period of study (*i.e.*, 1996 – 2006). The proxy ingredients used are correlated to the known major contributors to the TSI variation, namely sunspots and faculae. No physical meaning is attached to the regression coefficients and no attempt is made to study the actual contribution of the sunspots and faculae. We give for each of the composites (RMIB, PMOD, and ACRIM), the model for solar cycle 23, the RMS error of the residual (composite minus model), as well as the multiple coefficient of determination, R^2 (see Table 2 and Figures 8 – 10).

5. Model Comparisons

Each composite leads to a different model fit for solar cycle 23. The RMIB model exhibits the least RMS of the difference between measurements and model and the maximal coefficient of determination ($2\sigma = 0.304$ W m^{-2} and $R^2 = 0.93$). The residuals are larger at solar maximum than near the minimum, possibly owing to the influence of sunspots. See Figure 8.

The model computed from the PMOD composite over solar cycle 23 leads to ($2\sigma =$

Table 2 The three regression models.

RMIB	
RMIB model	$\mathrm{TSI}(t) = 1366.85 + 1.39 \times 10^{-3}\ \Sigma_{\mathrm{red}}(t) + 101\ \mathrm{Mg\,II}(t) - 0.447\ \mathrm{MPSI}(t)$
RMS of residuals	$0.152\ \mathrm{W\,m^{-2}}$
R^2	0.93
PMOD	
PMOD model	$\mathrm{TSI}(t) = 1365.95 + 1.57 \times 10^{-3}\ \Sigma_{\mathrm{red}}(t) + 82\ \mathrm{Mg\,II}(t) - 0.189\ \mathrm{MPSI}(t)$
RMS of residuals	$0.199\ \mathrm{W\,m^{-2}}$
R^2	0.86
ACRIM	
ACRIM model	$\mathrm{TSI}(t) = 1366.35 + 1.80 \times 10^{-3}\ \Sigma_{\mathrm{red}}(t) + 84\ \mathrm{Mg\,II}(t) - 0.004\ \mathrm{MPSI}(t)$
RMS of residuals	$0.31\ \mathrm{W\,m^{-2}}$
R^2	0.75

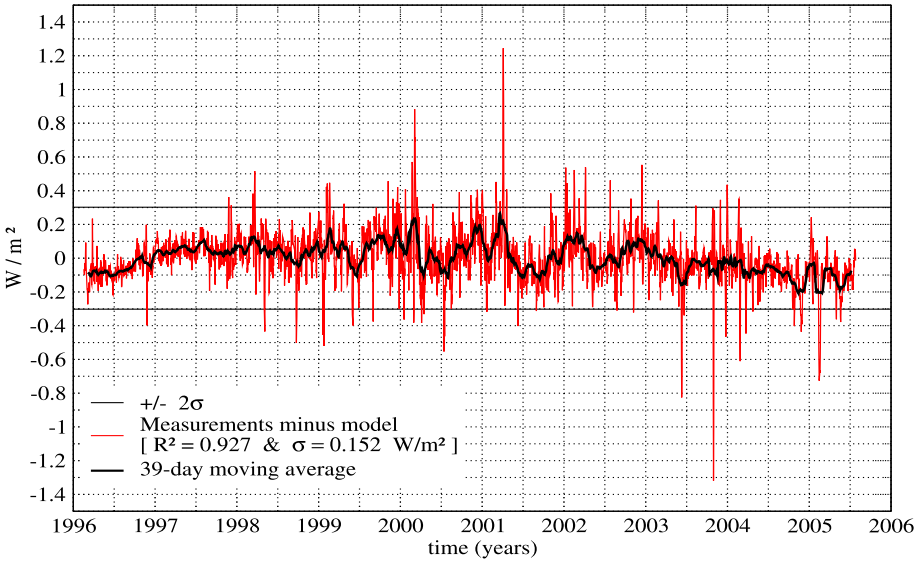

Figure 8 The residual of the RMIB regression model as a function of time (RMIB measurements minus RMIB model, red curve) and a 39-day moving average applied to residuals (bold black curve). The horizontal black lines indicate the $\pm 2\sigma$ interval of the red curve.

$0.4\ \mathrm{W\,m^{-2}}$ and $R^2 = 0.86$) with a downward linear trend in the residuals beginning in 2002 (Figure 9). The different behaviour from the RMIB composite can partly be explained by the additional changes applied to the data as the non-exposure-dependent corrections. The ACRIM composite leads to $2\sigma = 0.62\ \mathrm{W\ m^{-2}}$ and $R^2 = 0.75$ (Figure 10). The larger variability in the second part of the time series could be explained by the use of the ACRIM 3 data.

We shall now consider the RMIB composite regression model. In Figure 2 the 121-day running mean of this model is compared to the individual TSI instrument measurements.

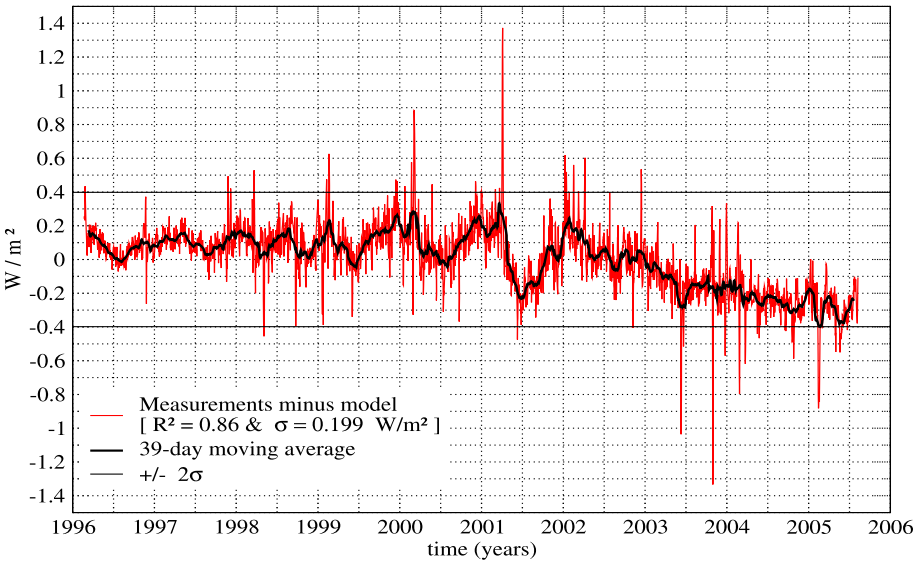

Figure 9 The residual of the PMOD regression model as a function of time (PMOD measurements minus PMOD model, red curve). The horizontal black lines indicate the $\pm 2\sigma$ interval of the red curve.

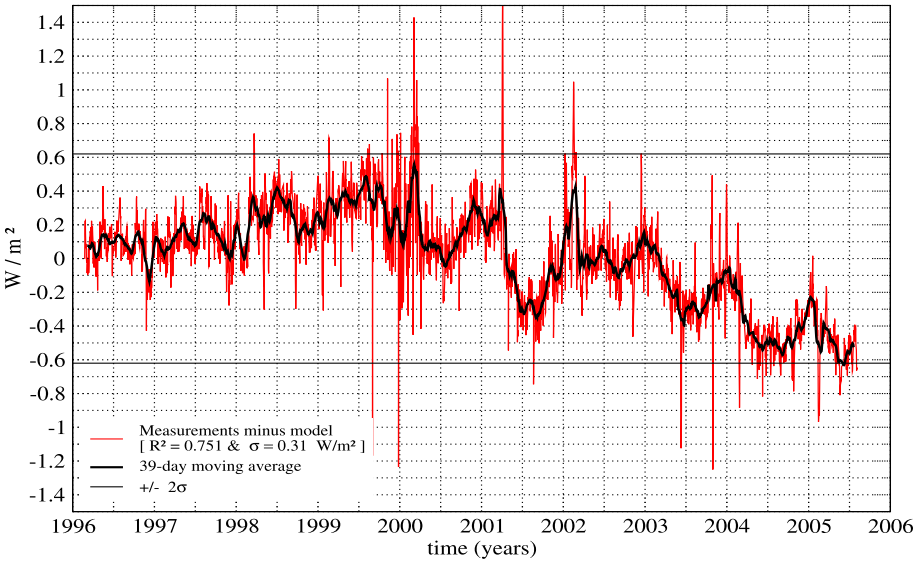

Figure 10 The residual of the ACRIM regression model as a function of time (ACRIM measurements minus ACRIM model, red curve). The horizontal black lines indicate the $\pm 2\sigma$ interval of the red curve.

Both the measurements and the model indicate that the minimal irradiance level has not been reached yet.

In Figure 4, the 121-day running mean of the RMIB model residual (green curve) is

compared to the difference between the VIRGO and the ACRIM2-ERBS-TIM composite (red curve), which was previously mentioned as providing an upper limit for the "internal error" of the RMIB composite. The vertical extent of the red curve is larger but of the same order of magnitude as that from the green curve. So the regression error is of the same order of magnitude as the error of the composite itself.

We suppose the different proxy indices will reach the same level as during the previous minimum (see Figures 5 – 7). Using constant model coefficients, we obtain a good fit ($2\sigma = 0.304$ W m^{-2} and $R^2 = 0.93$) between 1996 and 2006. We assume we will get an equally good representation of solar irradiance variability by keeping the constant coefficients up to 2008. We can conclude that the regression model assumes no variation of the solar minimum TSI.

Therefore the regression error with the extent of ± 0.14 W m^{-2} (see green curve, Figure 4) also provides the uncertainty with which we can measure that there is no change of solar minimum TSI during cycle 23. Such a conclusion implicitly assumes the used proxy indices – spots, faculae, and the chromospheric network – are the main factors responsible for TSI variability even in between solar minima. Nevertheless, a possible change in the TSI level between minima can arise from a nonmagnetic origin, such as a change in the effective temperature combined with diameter changes. Such effects if they exist could explain part of the residuals of the model or trend within the limit of instrumental stability (around 100 ppm).

We further test the stability of models parameters using solar cycle 22 measurements.

6. Solar Cycle 22 Reconstruction

From the RMIB model we have an estimate of the TSI values during solar cycle 22. Figure 11 displays the estimated TSI of solar cycle 22 from the model fit over solar cycle 23 data; the RMIB composite is also represented. A 39-day moving average is applied to both curves. The model fits well with data after 1990, but before 1990 the model overestimates the data by up to 0.4 W m^{-2} in 1986. This is better observed in Figure 12, where the residuals (difference between measurement and estimations) are shown. The $\pm 2\sigma$ interval covering solar cycles 22 and 23 is also plotted and shows that 96% of the residuals are spread between ± 0.44 W m^{-2}. For comparison the $\pm 2\sigma$ interval limited to solar cycle 23 residuals is also plotted. The disagreement between the reconstructed data and the measurements before 1990 can be explained by the lack of ageing correction capabilities on ERBS, which is the instrument that provided the measurements for this period. Therefore the new TSI composite time series is reproduced through the use of full-disc indices from ground-based measurement (MPSI and Σ_{red}) and one space-based record of Mg II. Theses indices display radiative variability owing to dark sunspots and faculae in the photosphere and bright plage and network in the chromosphere.

7. Conclusions

We have updated our SARR composite TSI time series from Dewitte *et al.* (2005) to obtain an accurate measurement of the TSI variation over cycle 23. We have considered all six instruments measuring TSI during the solar cycle, providing in total four time series (DIARAD, PMOV06, ERBS + TIM, and ACRIM2 + ACRIM3) of the TSI variation over the complete cycle.

Compared to Dewitte, Crommelynck, and Joukoff (2004), we have improved the DIARAD right shutter temperature determination. We have denoised the ERBS measurements

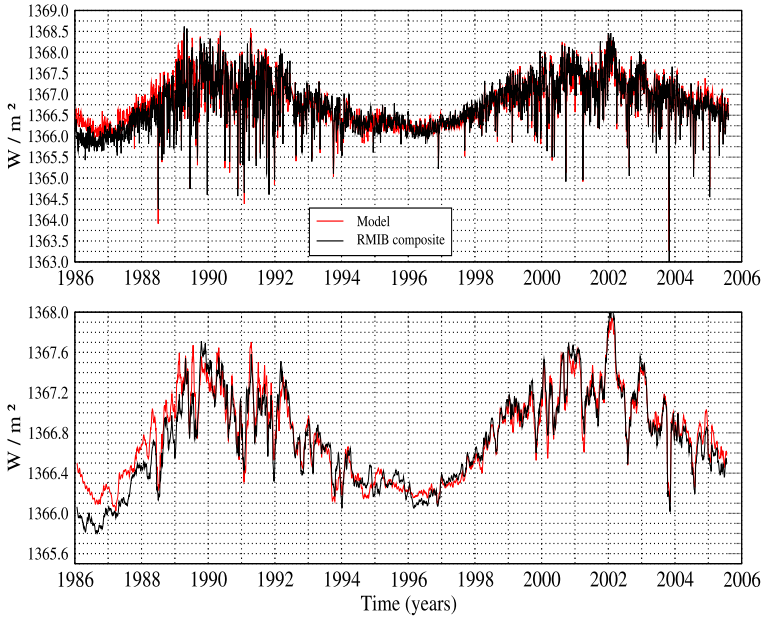

Figure 11 Reconstructed TSI for cycle 22 from cycle 23 model. Top panel: RMIB TSI composite times series (black curve) and the reconstructed time series for solar cycle 22 and 23 from the model determined over solar cycle 23 (red curve). Bottom panel: 39-day moving average of both time series.

(Equation (1)) such that they can be used as an independent data set for the long-term TSI variation.

We have brought all instruments to the same absolute level (Figure 2) by multiplication by an instrument-specific SARR adjustment coefficient (Table 1). ACRIM3 descends more quickly than the other radiometers during the descending phase of the cycle. Our new composite is the average of all other SARR-adjusted radiometers (DIARAD, PMOV06, denoised ERBS, TIM, and ACRIM2). The uncertainty of this composite is estimated to be lower than ± 0.2 W m^{-2} over the entire solar cycle 23, and lower than ± 0.05 W m^{-2} from 2003 onwards.

Alternative composite TSI time series for cycle 23 are those from Fröhlich (2003), which uses the VIRGO radiometers (DIARAD and PMOV06) with exposure-independent corrections, and the one from Willson and Mordvinov (2003), which uses the ACRIM 2 and 3 radiometers.

We have determined for each of the available composite time series an empirical model for solar cycle 23 using the Mg II core-to-wing ratio, Σ_{red}, and the magnetic plage strength indices. Such a model is unable to separate the contributions from active regions, spots, and faculae, but it can be used to assess the precision and reproducibility of the measurements.

We found a better model fit for the RMIB composite than for PMOD and ACRIM in terms of root mean square of the residuals (measurements minus model), the residuals being within ± 0.304 W m^{-2} (2σ errors) over solar cycle 23, with R^2 of the order of 0.93. For the PMOD TSI composite time series the model leads to a 2σ interval of order of 0.4 W m^{-2}, $R^2 = 0.86$. An unexplained linear trend of the order of 0.4 W m^{-2} from 2002 to 2006 is observed in the residual, which corresponds to about 0.1 W m^{-2} per year. A model fitted to ACRIM composite data for solar cycle 23 gives residuals within ± 0.61 W m^{-2} and $R^2 = 0.75$. As a

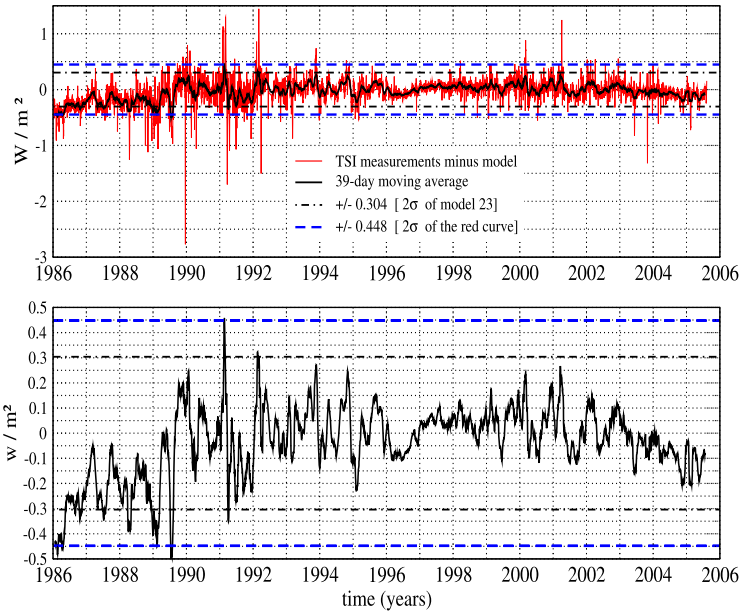

Figure 12 RMIB TSI composite minus model extrapolated to cycle 22. Top panel: The difference between the RMIB TSI composite times series and the reconstructed time series for solar cycles 22 and 23 from the model determined over solar cycle 23 (red curve) and 39-day moving average (black curve) of the red curve. The 2σ interval computed in Section 4 for solar cycle 23 is also displayed (black dots) as well as the 2σ interval of the residuals for solar cycles 22 and 23 (blue curve). Bottom panel: Magnification of the top panel between ± 0.5 W m^{-2} where only the 39-day moving average is displayed.

consequence the RMIB model is used to reconstruct the solar irradiance during solar cycle 22 with residuals errors mostly within ± 0.44 W m^{-2} (2σ error). The model overestimates the measurement before 1990; a possible explanation for this could be the lack of ageing monitoring capability of ERBS.

From the comparison of the RMIB composite and its proxy regression model, we can expect that the solar minimum TSI will not change during cycle 23 with an uncertainty of ± 0.14 W m^{-2}. We assume the proxy indices and particularly the Mg II component will reach the same level as during the previous minimum. We assume also that the parameters of the model remain through at least 2008. This is a reduction in uncertainty compared to cycle 22, where we found a TSI minimum variation of 0.15 ± 0.35 W m^{-2} (Dewitte *et al.*, 2005).

For the future we can expect a further reduction in uncertainty if the DIARAD, PMOV06, and TIM radiometers – which agree within ± 0.05 W m^{-2} – are continued. The continuation of DIARAD and PMOV06 is foreseen with the instruments Solar Variability Picard (SOVAP) and Precision Monitoring Sensor (PREMOS) on the *Picard* satellite (Thuillier *et al.*, 2006), slated for launch in March 2009; the continuation of TIM is foreseen on the *Glory* satellite, which will be launched in December 2008.

Acknowledgements We thank the science groups for making their data available and particularly S.R. Walton from the San Fernando Observatory. We thank the radiometry team of the Royal Meteorological Institute of Belgium and A. Ipe and N. Clerbaux from the GERB team for helpful discussions. We acknowledge the efforts of the VIRGO investigation on SOHO, a cooperative ESA/NASA Mission. This study includes data from the synoptic program at the 150-foot solar tower of the Mt. Wilson Obervatory. The Mt. Wilson 150-foot solar tower is operated by UCLA, with funding from NASA, ONR, and NSF, under agreement with the

Mt. Wilson Institute. This work was supported by Belgian Science Policy office through the ESA PRODEX program.

References

Crommelynck, D.: 1982, In: Hall, J.B. Jr. (ed.) *Earth Radiation Science Seminars, NASA Conf. Publ.* **2239**, 53.
Crommelynck, D., Domingo, V.: 1984, *Science* **225**, 180.
De Toma, G., White, O.R., Chapman, G.A., Walton, S.R.: 2004, *Adv. Space. Res.* **34**, 237.
Dewitte, S., Crommelynck, D., Joukoff, A.: 2004, *J. Geophys. Res.* **109**, A02102.
Dewitte, S., Crommelynck, D., Mekaoui, S., Joukoff, A.: 2005, *Solar Phys.* **224**, 209.
Foukal, P., Fröhlich, C., Spruit, H., Wigley, T.M.L.: 2006, *Nature* **443**, 14.
Fröhlich, C.: 2003, *Metrologia* **40**, 60.
Fröhlich, C.: 2004, *Presented at AGU Fall Meeting*. ftp://ftp.pmodwrc.ch/pub/Claus/AGU-Fall2004.
Fröhlich, C., Lean, J., 1998, *Geophys. Res. Lett.* **25**, 4377.
Preminger, D.G., Walton, S.R., Chapman, G.A.: 2002, *J. Geophys. Res.* **107**, 1354.
Thuillier, G., Dewitte, S., Schmutz, W., PICARD team: 2006, *Adv. Space Res.* **38**, 1792.
Viereck, R.A., Puga, L.C., Lawrence, C.: 1999, *J. Geophys. Res.* **104**, 9995.
Viereck, R.A., Puga, L., McMullin, D., Judge, D., Weber, M., Tobiska, W.K.: 2001, *Geophys. Res. Lett.* **28**, 1343.
Walton, S.R., Cookson, A.M., Perminger, D.G., Chapman, G.A.: 2004, *Presented at AGU Fall Meeting*, SH53A-0303.
Willson, R.C., Mordvinov, A.: 2003, *Geophys. Res. Lett.* **30**, 1199.